

Post irradiation plastic properties of F82H derived from the instrumented tensile tests [☆]

T. Taguchi ^{a,*}, S. Jitsukawa ^b, M. Sato ^c, S. Matsukawa ^c, E. Wakai ^b, K. Shiba ^b

^a Neutron Science Research Center, Japan Atomic Energy, Research Institute, Tokai-Mura, Ibaraki-Ken 319-1195, Japan

^b Department of Materials Science, Japan Atomic Energy, Research Institute, Tokai-Mura, Ibaraki-Ken 319-1195, Japan

^c KKS, JFE, Kawasaki-Ku, Kawasaki-Shi, Kanagawa-Ken 210-0855, Japan

Received 23 April 2004; accepted 4 August 2004

Abstract

F82H (Fe–8Cr–2W) and its variant doped with 2%Ni were irradiated up to 20dpa at 300 °C in the High Flux Isotope Reactor (HFIR) at Oak Ridge National Laboratory. Post irradiation tensile testing was performed at room temperature. During testing, the images of the specimens including the necked region were continuously recorded. Tests on cold worked material were also carried out for comparison. From the load–displacement curves and the strain distributions obtained from the images, flow stress levels and strain hardening behavior was evaluated. A preliminary constitutive equation for the plastic deformation of irradiated F82H is presented. The results suggest that the irradiation mainly causes defect-induced hardening while it did not strongly affect strain hardening at the same flow stress level for F82H irradiated at 300 °C. The strain hardening of Ni doped specimens was, however, strongly affected by irradiation. Results provide basics to determine allowable stress levels at temperatures below 400 °C.

© 2004 Elsevier B.V. All rights reserved.

1. Introduction

At temperatures below 350 °C, reduced activation martensitic steels exhibit hardening under neutron irradiation. Yield stress often increases by >50% and uniform elongation reduces to zero. Available structural design criteria, such as ASME Sec. III, RCC-MR and MITI-501, assume that uniform elongation is not lim-

ited [1]. This criterion may not be met for irradiation hardened steels. To obtain structural design methodology applicable for irradiation hardened steels, it is essential to understand the effect of irradiation on the plastic properties including ductile fracture condition of the alloys. Ductile fracture conditions without irradiation effects have been examined through research on deformation during metal forming [2–5]. It has been shown that the ductile fracture condition is controlled by strain hardening capability and the triaxiality of the stress. Therefore, the effect of irradiation on the strain hardening capability is evaluated. The strain hardening capability was obtained from the relation of flow stress and the plastic strain.

To obtain the flow stress and the plastic strain relation of irradiation hardened reduced activation

[☆] Originally this work was presented at 11th International Conference on Fusion Reactor Materials (ICFRM-11).

* Corresponding author. Tel.: +81 29 282 5497; fax: +81 29 282 5922.

E-mail address: taguchi@popsvr.tokai.jaeri.go.jp (T. Taguchi).

martensitic steels, the engineering stress–strain data were obtained by measuring the neck geometry during tensile testing. From the results, approximate true flow stress–plastic strain relation of irradiated alloy is obtained. This was also carried out for cold worked specimens. The effect of irradiation on the strain hardening characteristics is discussed.

2. Experimental procedure

A reduced activation martensitic steel of F82H with 0.1C–7.8Cr–2W–0.04Ta–Fe(bal.) and its variant doped with 2%Ni were tested. F82H (IEA-F82H) and 2%Ni doped F82H were normalized at 1040°C for 1 h. They were subsequently tempered at 750°C for 1 h and at 720°C for 1 h, respectively. Tensile specimens of the alloys were irradiated in HFIR in Oak Ridge at 300°C to 5 dpa (RB-11J capsule) and 20 dpa (JP25 capsule). Specimens were also taken from the cold worked plates of F82H after 70% and 80% reduction (tensile direction was parallel to the rolling direction). Plate tensile specimens 25.4 mm long and 0.76 mm thick was used. The gage region of the specimen was 7.5 mm long and 1.5 mm wide.

All tests were performed at ambient temperature in the Hot Cell of the JMTR at JAERI. During the test, load–displacement data were recorded. Also, the gage section imaging was carried out with a CCD camera (1M or higher pixels). For unirradiated specimens, images including width and thickness of the specimens were recorded (location of the cameras and a specimen image are shown in Fig. 1). Only the images for width were obtained for irradiated specimens.

3. Experimental results

Engineering stress–strain relations from IEA-F82H and 2% Ni doped F82H specimens irradiated to 0, 5

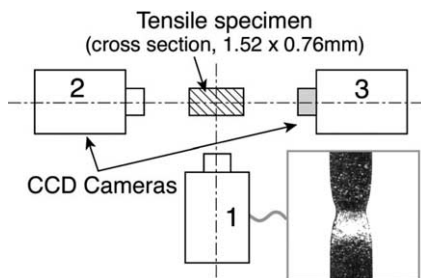


Fig. 1. Positions of CCD cameras. To measure the strain distribution in the neck in the gage section of the specimen, the images of the specimens have been recorded continuously during the tensile test. Tensile direction is perpendicular to the sheet.

and 20 dpa are shown in Fig. 2. The strain to necking (STN; corresponds to uniform elongation for unirradiated specimens) decreased to zero by irradiation to 5 dpa. STN for 2% Ni-doped F82H specimens also decreased to zero after irradiation to 5 dpa. Yield stress of Ni-doped specimen was relatively large after irradiation; yield stress levels before and after irradiation were 740 and 1400 MPa, respectively.

The area at the minimum cross section of the specimen during the tensile test was evaluated from the image of the neck. From the area during testing and the engineering stress–strain relation, mean tensile stress and the strain relation at the minimum cross section has been obtained. This relation is referred to as the uncorrected true stress strain relation $Ts-s/u$ in the following (to obtain the relation between flow stress and plastic strain, it is required to evaluate the stress concentration by the neck configuration). The results are seen in Fig. 3. The strain in thickness direction was slightly larger than that in width direction in the strain range for neck development. The relation obtained from only width strain supposing the strains in width and thickness direction ($Ts-s/uw$) were identical are also shown in Fig. 3; the deviations were not large even at strains near fracture.

Because of the limited ability for the image recording during testing, strain at the neck was estimated only from the deformation along the width direction for irradiated specimens. $Ts-s/uw$ curves for IEA-F82H specimens and 2% Ni-doped specimens irradiated to 0 and 5 dpa are shown in Fig. 4. These results indicate the positive true strain-hardening rate during necking deformation in both irradiated and cold worked specimens. This tendency corresponds to previous works [6–13].

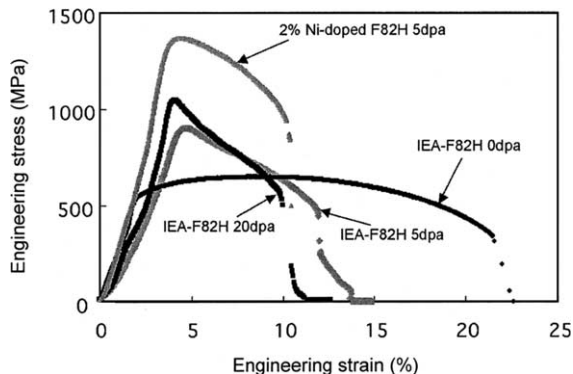


Fig. 2. Engineering stress and strain relations before and after irradiation. Curves for the specimens of IEA-F82H irradiated to 20 dpa and that for 2% Ni-doped specimen irradiated to 5 dpa are shown.

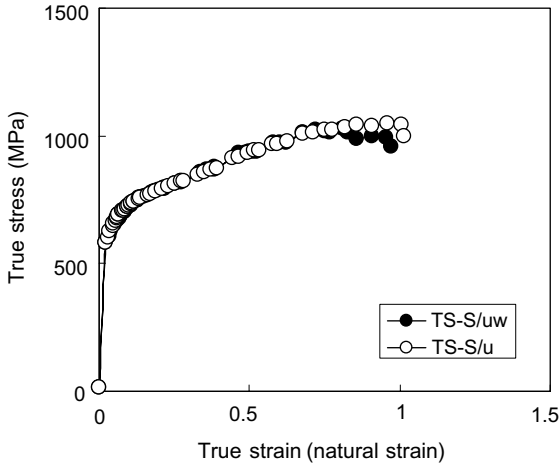


Fig. 3. Uncorrected true stress–strain relations of irradiated and unirradiated specimens. Ts–s/u stands for the strain at the minimum cross section estimated from the neck profile obtained with CCD cameras 1, 2 and 3 (see, Fig. 1), while Ts–s/uw stands for that obtained by CCD camera 1 only. For irradiated specimen, only CCD camera 1 was used for the image recording.

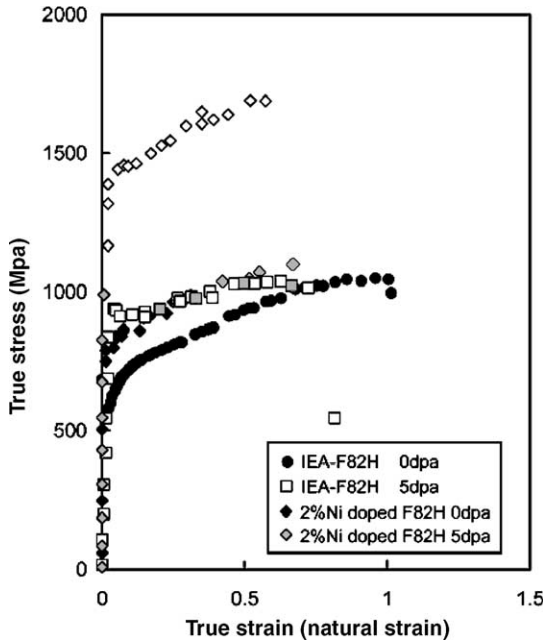


Fig. 4. Uncorrected true stress–strain relations for IEA-F82H and Ni doped F82H irradiated to 5dpa. The curve for IEA-F82H before irradiation was also plotted. Strain hardening capability for irradiated IEA-F82H was decreased by irradiation, although residual ductility after irradiation maintains a high level. Ni doped specimen exhibited a large flow stress value after irradiation, while strain hardening capability was little affected by irradiation.

4. Discussion

4.1. Effect of specimen configuration (*w/t*) on fracture strain

Ductile fracture strain of a plate under tensile loading depends on the stress triaxiality and the strain hardening rate $d\sigma/d\varepsilon$ (or strain hardening exponent n), as shown in Fig. 5. Fracture strain attains maximum under equibiaxial tensile condition (A in the figure) and uniaxial tensile condition with neck development (A' in the figure corresponding to tensile deformation of a round bar and that with square cross section); in case the plastic behavior is expressed by $\sigma = Ae^n$, fracture strain attains a maximum value of $2n$ or slightly higher with $d\sigma/d\varepsilon$ of about half of the instantaneous stress level, $\sigma/2$ (see Fig. 5). However, fracture strain becomes slightly larger with strain rate sensitivity of flow stress. Minimal value of the fracture strain appears under uniaxial tension without neck development (deformation along the y axis in the figure, as indicated by an arrow B) when the $d\sigma/d\varepsilon$ is of about the instantaneous stress level, σ . The stress state at the neck region of plate tensile specimen is between A' and B in Fig. 5. With higher w/t , the stress state becomes close to that along the y axis. During neck development (plastic) strain rate in thickness direction becomes higher than that in the width direction for the specimen with $w/t > 1$. Therefore, stress state at neck shifts from A' to B with deformation.

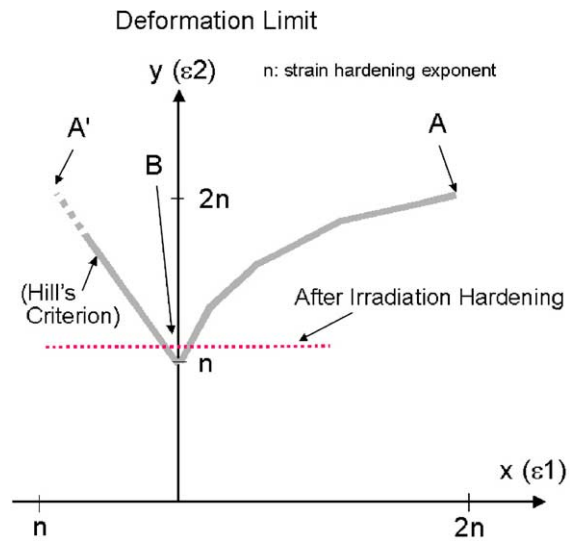


Fig. 5. Deformation limit diagram (ductile fracture condition). Deformation limit for equi-biaxial stretching attains $2n$, while that for uniaxial plane strain stretching ($\varepsilon_1 = 0$) attains only n (n stands for strain hardening exponent).

4.2. True stress strain relation $Ts-s/u$ of cold worked specimen

Flow stress is thought to be a function of plastic strain ε (σ increases monotonically with strain in most cases).

$$\sigma = f(\varepsilon).$$

Therefore, the relation for cold worked specimen may be expressed by

$$\sigma = f(\varepsilon_0 + \varepsilon),$$

where ε_0 corresponds to the plastic strain introduced during cold working. This indicates that the curves ($Ts-s/u$) for cold worked specimens may be superimposed by shifting along the x -axis on that before cold working. Fig. 6 apparently shows that the curves are well overlapped. The shift (plastic strain) corresponds to the equivalent strain for the hardening by cold working.

Fracture strains ($\varepsilon_0 + \varepsilon$) for cold worked specimens are slightly larger than that before cold working, as seen in the figure. This resulted from the fact that fracture condition for the specimen without cold working was rather close to condition B in Fig. 5 (see Section 4.1).

4.3. True stress strain relation estimated from the width strain $Ts-s/w$

Because of the limited ability, strain at the minimum cross section for irradiated specimens was estimated from the strain only in the width direction. $Ts-s/w$ is compared with $Ts-s/u$ to evaluate the deviation.

No large disagreement exists between $Ts-s/w$ and $Ts-s/u$ for the specimen before cold working (see Fig. 3).

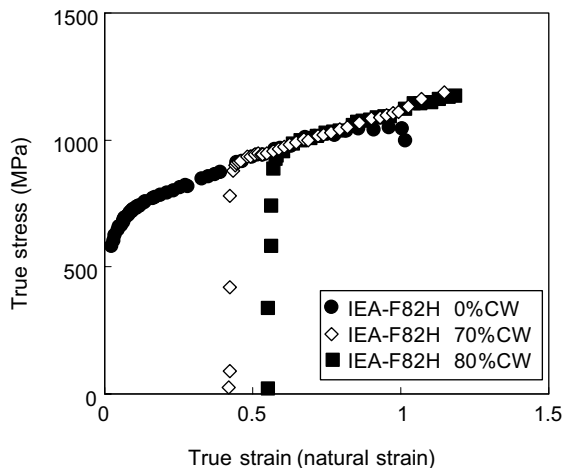


Fig. 6. Uncorrected true stress–strain relations of cold worked specimens. Specimens were cold worked to 70 and 80% reduction.

However, the anisotropy in width and thickness direction was introduced by cold working.

4.4. True stress strain ($Ts-s/w$) for the specimens before and after irradiation

$Ts-s/w$ for irradiated (to 5 and 20 dpa) specimens are superimposed by shifting along the x -axis with that for unirradiated specimen, as seen in Fig. 7. This suggests that irradiation mainly increases the equivalent strain (ε_0) corresponding to hardening in the constitutive equation, as has been indicated for irradiation hardened austenitic steel [10]. This also suggests that plastic behavior including the ductile fracture condition of irradiated specimens may be approximated by cold worked specimens, as far as monotonic and static plastic deformation is concerned. It should also be pointed out that residual ductility was not small even for the specimen irradiated to 20 dpa; about half of that for before irradiation, as seen in Fig. 7. Previous works also reported the similarity between the strain hardening behaviors of irradiated and cold worked specimens [7,11,13].

4.5. Irradiation effects on $Ts-s/w$ of 2%Ni doped specimens

$Ts-s/w$ curves for unirradiated and irradiated 2%Ni-doped specimens are shown in Fig. 4. Unlike those for IEA-F82H specimens (see Figs. 4 and 7), the curve could not be superimposed by shifting along the x -axis. This implies that irradiation affected the self-energy of dislocations or increased friction to dislocation motion for the Ni-doped heat. This effect may be interpreted as an extra effect due to the radiation induced precipitation of very fine particles (very fine voids or hard particles), which might pin down dislocations.

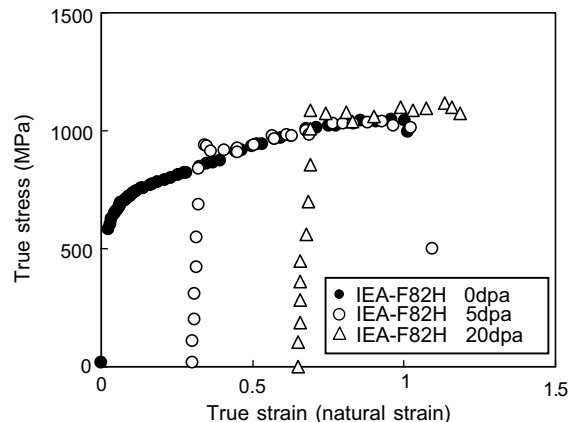


Fig. 7. Uncorrected true stress–strain relations of irradiated (to 5 and 20 dpa) and unirradiated IEA-F82H. The curves for irradiated specimens are superimposed well with that for the unirradiated specimen by shifting along the x -axis.

5. Summary

- (1) Approximate true stress and strain relations of unirradiated and irradiated specimens were obtained from engineering stress and strain relations with measurement of the neck development during tensile testing.
- (2) The approximate true stress and strain curves for irradiated specimens of the reduced activation heat IEA-F82H are superimposed with that for unirradiated specimen by shifting along the x -axis. This indicates that irradiation mainly increased the equivalent strain (ϵ_0) corresponding to the hardening at zero strain in the constitutive equation.
- (3) This also suggests that plastic behavior including ductile fracture condition of irradiated specimen may be approximated by cold worked specimens, as far as monotonic and static plastic deformation is concerned. It should also be pointed out that residual ductility was not small even after irradiation to 20 dpa.
- (4) The curves for specimens of Ni-doped heat before and after irradiation could not be superimposed. This implies that irradiation affected self-energy of dislocations or increased friction to dislocation motion of the heat.

References

- [1] S. Majumdar, P. Smith, Fusion Eng. Des. 41 (1998) 25.
- [2] R. Hill, J. Mech. Phys. Solids 1 (1952) 19.
- [3] R. Hill, J.W. Hutchinson, J. Mech. Phys. Solids 23 (1975) 239.
- [4] H.W. Swift, J. Mech. Phys. Solids 1 (1952) 1.
- [5] A.K. Ghosh, in: D.P. Koistinen, N.M. Wang (Eds.), Mechanics of Sheet metal forming, Plenum, New York, 1978, p. 287.
- [6] A. Hishinuma, S. Jitsukawa, J. Nucl. Mater. 169 (1989) 241.
- [7] S. Jitsukawa, M.L. Grossbeck, A. Hishinuma, J. Nucl. Mater. 179–181 (1991) 563.
- [8] S. Jitsukawa, M.L. Grossbeck, A. Hishinuma, J. Nucl. Mater. 191–194 (1992) 790.
- [9] R.J. DiMelfi, D.E. Alexander, L.E. Rehn, J. Nucl. Mater. 252 (1998) 171.
- [10] S. Jitsukawa, I. Ioka, A. Hishinuma, J. Nucl. Mater. 271&272 (1999) 167.
- [11] E.V. van Osch, M.I. de Vries, J. Nucl. Mater. 271&272 (1999) 162.
- [12] A. Deschamps, M. Militzer, W.J. Poole, ISIJ Int. (Japan) 41 (2) (2001) 196.
- [13] T.S. Byun, K. Farrell, Acta Mater. 52 (2004) 1597.